



Published in final edited form as:

Cell Microbiol. 2013 September ; 15(9): . doi:10.1111/cmi.12137.

A Key Role for Lipoic Acid Synthesis During *Plasmodium* Liver stage Development

Brie Falkard¹, T. R. Santha Kumar¹, Leonie-Sophie Hecht², Krista A. Matthews³, Philipp P. Henrich¹, Sonia Gulati¹, Rebecca E. Lewis¹, Micah J. Manary⁴, Elizabeth A. Winzeler⁴, Photini Sinnis³, Sean T. Prigge³, Volker Heussler^{2,5}, Christina Deschermeier², and David Fidock^{1,6,*}

¹Department of Microbiology and Immunology, Columbia University Medical Center, New York, NY, USA ²Bernhard-Nocht-Institute for Tropical Medicine, Department of Molecular Parasitology, Hamburg, Germany ³Department of Molecular Microbiology & Immunology, Johns Hopkins Bloomberg School of Public Health, Baltimore, MD, USA ⁴Department of Pediatrics, University of California San Diego, La Jolla, CA, USA ⁵Institute of Cell Biology, University of Bern, Switzerland ⁶Division of Infectious Diseases, Department of Medicine, Columbia University Medical Center, New York, NY, USA

SUMMARY

The successful navigation of malaria parasites through their life cycle, which alternates between vertebrate hosts and mosquito vectors, requires a complex interplay of metabolite synthesis and salvage pathways. Using the rodent parasite *Plasmodium berghei*, we have explored the synthesis and scavenging pathways for lipoic acid, a short-chain fatty acid derivative that regulates the activity of α -ketoacid dehydrogenases including pyruvate dehydrogenase. In *Plasmodium*, lipoic acid is either synthesized *de novo* in the apicoplast or is scavenged from the host into the mitochondrion. Our data show that sporozoites lacking the apicoplast lipoic acid protein ligase LipB are markedly attenuated in their infectivity for mice, and *in vitro* studies document a very late liver stage arrest shortly before the final phase of intra-hepatic parasite maturation. LipB-deficient asexual blood stage parasites show unimpaired rates of growth in normal *in vitro* or *in vivo* conditions. However, these parasites showed reduced growth in lipid-restricted conditions induced by treatment with the lipoic acid analog 8-bromo-octanoate or with the lipid-reducing agent clofibrate. This finding has implications for understanding *Plasmodium* pathogenesis in malnourished children that bear the brunt of malarial disease. This study also highlights the potential of exploiting lipid metabolism pathways for the design of genetically attenuated sporozoite vaccines.

Keywords

Plasmodium berghei; lipoic acid; apicoplast; transfection; clofibrate

INTRODUCTION

Despite recent reductions in its morbidity and mortality, malaria afflicts over 220 million and kills over 600,000 individuals each year (WHO, 2012). Infection begins with a small inoculum of *Plasmodium* sporozoites (thought to be <100; (Medica and Sinnis, 2005)) that

*Correspondence: df2260@columbia.edu; Tel. (+1) 212-305-0816; Fax: (+1) 212-305-4038.

All authors hereby confirm that they have no conflict of interest in the publication of this research.

are delivered into the host dermis during the bloodmeal of a female *Anopheles* mosquito (Amino *et al.*, 2006; Yamauchi *et al.*, 2007). These sporozoites rapidly migrate to and infect host hepatocytes, where they begin to divide at one of the fastest rates of cell division known for any eukaryotic cell (Graewe *et al.*, 2012). This amplification event generates thousands of daughter parasites that burst from the infected hepatocytes and invade red blood cells (RBCs), initiating the pathogenic asexual blood stage cycle (Silvie *et al.*, 2008). The clinically silent nature of liver stage infection, its low numbers of infected cells, and the existence of MHC-mediated antigen presentation in the hepatocyte host cell, make this a very attractive target for the development of vaccines or chemoprophylactic agents (Prudencio *et al.*, 2006) that prevent the onset of clinical manifestations.

To meet the prodigious metabolic demands associated with the high multiplication rate in the liver, *Plasmodium* parasites up-regulate a series of *de novo* synthesis pathways including type II fatty acid biosynthesis (FAS-II; (Tarun *et al.*, 2008)). The FAS-II pathway generates an eight-carbon chain precursor (octanoic acid) that is used for the synthesis of lipoic acid (6,8-thioctic acid), a cyclic disulphide-containing derivative of octanoic acid that is an essential cofactor for a number of multi-enzyme complexes found in almost all eukaryotic cells (Spalding *et al.*, 2010a; Goraca *et al.*, 2011). In addition to being synthesized *de novo*, lipoic acid can also be absorbed from dietary sources. Cells maintain active systems to scavenge non-protein bound lipoic acid from their environment (Biewenga *et al.*, 1997; Shay *et al.*, 2009).

In *Plasmodium*, covalently attached lipoic acid regulates the function of three α -ketoacid dehydrogenases, namely pyruvate dehydrogenase (PDH), α -ketoglutarate dehydrogenase (KGDH) and branched-chain α -ketoacid dehydrogenase (BCDH). These multi-enzyme complexes contribute to amino acid and energy metabolism and consist of multiple copies of a substrate-specific α -ketoacid decarboxylase (the E1 subunit), an acyltransferase (the E2 subunit) and a dihydrolipoamide dehydrogenase (the E3 subunit) (Storm and Muller, 2012). These α -ketoacid dehydrogenases generally convert an α -ketoacid, NAD^+ and coenzyme A (CoA) to CO_2 , NADH and acyl-CoA. E2 subunits include a lipoyl domain that when bound to lipoic acid acts as a swinging arm to transfer reaction intermediates between E1, E2 and E3. Lipoic acid is also attached to the H-protein, a component of the glycine cleavage system that reversibly decarboxylates glycine (Storm and Muller, 2012). PDH, comprised of the lipoylated subunit E2 as well as subunits E1 and E3, is located in the parasite apicoplast, a plastid-like organelle that performs a variety of metabolic functions including isoprenoid and fatty acid biosynthesis (Ralph *et al.*, 2004; Foth *et al.*, 2005). In the apicoplast, PDH is thought to catalyze the oxidative decarboxylation of pyruvate to generate acetyl-CoA (Pei *et al.*, 2010). In contrast to PDH-E2, the other lipoylated proteins (KGDH-E2, BCDH-E2 and the H-protein) have been localized to the mitochondria (Gunther *et al.*, 2005; Spalding and Prigge, 2010b). In this organelle, KGDH is believed to catalyze the oxidative decarboxylation of α -ketoglutarate to succinyl-CoA as an integral part of the TCA cycle, whereas BCDH is involved in the degradation of the branched-chain amino acids valine, leucine and isoleucine (Storm and Muller, 2012).

Plasmodium parasites synthesize lipoic acid within the apicoplast, where the FAS-II pathway produces octanoic acid attached to acyl-carrier protein (ACP) as one of its products (Gunther *et al.*, 2007). The derivation of lipoic acid from octanoyl-ACP requires two apicoplast-targeted enzymes: octanoyl-ACP transferase (LipB) and lipoate synthase (LipA). LipB transfers the octanoyl group to a lipoyl-accepting domain, whereas LipA is responsible for catalyzing the introduction of two sulphurs at positions 6 and 8, forming the lipoyl group (Fig. 1A). LipA is capable of generating lipoic acid from the octanoyl-ACP precursor before or after its transfer by LipB, although it is thought that LipA prefers the E2 protein-bound substrate. In the apicoplast, these enzymes mediate the attachment of lipoic acid to PDH-E2

(Wrenger and Muller, 2004). In the human parasite *P. falciparum*, *LipB* was earlier shown to be important for lipoylating PDH-E2 but was itself nonessential to blood stage replication (Gunther *et al.*, 2007). In that study, LipB-deficient (Pf LipB) parasites were reported to have an increased growth rate during the asexual blood stages, a reduced level of lipoylated PDH-E2 protein, and a reduction in the total lipoic acid content in the parasite. The lipoate protein ligase LplA2, which is apparently targeted to both the apicoplast and the mitochondria, was hypothesized to compensate for the loss of *PfLipB* function and to account for the residual PDH-E2 lipoylation that was observed in those knockout (KO) parasites (Gunther *et al.*, 2007).

In addition to the lipoic acid synthesis pathway, *Plasmodium* parasites have an active scavenging pathway that appears to be essential for both blood- and liver stage development and that has been shown to lead to lipoylation of KGDH-E2, BCDH-E2 and the H-protein in the mitochondrion (Allary *et al.*, 2007; Deschermeier *et al.*, 2012). Host lipoic acid may be imported via the parasite pantothenate transporter (Saliba and Kirk, 2001; Kirk and Saliba, 2007; Spalding *et al.*, 2010b). Scavenged radiolabeled lipoic acid was found to sequester solely in the mitochondrion and appeared to be attached to these proteins by the action of lipoic acid protein ligase LplA1 (Allary *et al.*, 2007). This enzyme can also ligate the lipoic acid analog 8-bromo-octanoate (8-BOA), an antimetabolite that is thought to compete with lipoic acid as a substrate, thereby inhibiting lipoylation of mitochondrial target proteins by irreversibly attaching to their E2 subunits and inactivating the multi-component complexes (Crawford *et al.*, 2006; Allary *et al.*, 2007). Addition of 8-BOA to *P. falciparum* asexual blood stage or *P. berghei* liver stage parasites cultured *in vitro* affected their growth in a dose-dependent manner (Allary *et al.*, 2007; Deschermeier *et al.*, 2012). The synthesis and scavenging pathways have generally been considered to operate separately, with no lipoic acid exchange occurring between the mitochondrion and apicoplast organelles (Allary *et al.*, 2007; Gunther *et al.*, 2009).

While the studies with *PfLipB* suggest that its role in *de novo* lipoic acid synthesis is not required for blood stage growth (Gunther *et al.*, 2007), no study to date has investigated its requirement for rapid liver stage growth. The observation that LipA expression is upregulated during early liver stage development in the rodent parasite *P. yoelii* nevertheless suggests an important role for *de novo* synthesis (Tarun *et al.*, 2008). Indeed, *P. yoelii* parasites engineered to lack the PDH complex (whose functionality is dependent on E2 lipoylation) were unaffected in their kinetics of blood stage replication in mice yet were severely attenuated during the liver stage (Pei *et al.*, 2010).

In this study, we have disrupted the *P. berghei LipB* gene to determine its essentiality throughout the parasite life cycle. Our studies reveal that parasites lacking *PbLipB* progress unimpeded through the asexual and sexual blood stages in normal mice and develop normally in the mosquito, but fail to mature properly during the liver stage both *in vivo* and *in vitro*, indicating a key requirement for lipoic acid synthesis during intra-hepatic replication. We also identify an important role for this synthesis pathway during asexual blood stage replication in host environments whose exogenous lipid levels have been diminished, either through the use of lipid-lowering drugs or via 8-BOA mediated blockage of the lipoic acid scavenging pathway.

RESULTS

Disruption of the LipB gene in *P. berghei*

To monitor the effect of disrupting lipoic acid synthesis in *Plasmodium* parasites, we chose *LipB* that is known to be non-essential for asexual blood stage proliferation in *P. falciparum* (Gunther *et al.*, 2007), and performed disruption studies in the rodent species *P. berghei*

(ANKA strain) in order to examine the entire life cycle. We first constructed the pL0001-*PbLipB* plasmid that carried the *Toxoplasma gondii dhfr-ts* selection cassette flanked by 5 and 3 untranslated regions (UTRs) from the *PbLipB* locus. A linearized DNA fragment containing the selection cassette flanked by the targeting sequences was then electroporated into *P. berghei* asexual blood stage parasites. Transformed parasites were selected using pyrimethamine. Double crossover events between the plasmid and genomic regions of homology were predicted to result in deletion of *PbLipB* and its replacement by the *dhfr-ts* marker (Fig. 1B; primer locations listed in Table S1). This was confirmed by PCR assays conducted with cloned *Pb LipB* knockout (KO) parasites and the parental ANKA wild-type (WT) strain (Fig. 1C). The loss of *PbLipB* expression in these KO parasites was also confirmed by RT-PCR with primers specific to the *LipB* coding sequence. These assays identified *PbLipB* transcripts in liver and asexual blood stages in WT parasites but not in the *Pb LipB* clone (Fig. 1D).

***P. berghei* LipB-deficient parasites maintain normal asexual blood stage growth rates and apicoplast development**

Earlier studies in *P. falciparum* reported a modestly increased rate of proliferation in asexual blood stage parasites carrying a disruption in the *LipB* gene. This was attributed to a slight decrease in the cell cycle duration (Gunther *et al.*, 2007). To test for a similar phenotype in *P. berghei*, we intravenously inoculated either 10,000 or 1,000 asexual blood stage parasites from either *Pb LipB* or WT parasites into Swiss-Webster mice and monitored their parasitemia daily by blood smears. Results from three independent experiments (with 5 mice per strain per experiment) showed no significant differences in growth rates at either starting inocula (Fig. 2A, 2B).

To further characterize the phenotype of *Pb LipB* parasites during the blood stages, we assessed the morphology of the apicoplast, the site of lipoic acid synthesis. This organelle undergoes a striking morphological change over the course of blood stage development. Beginning as a compact dot in the ring stage, the apicoplast grows during schizogony into a highly branched structure that then segregates into individual daughter cells (merozoites), ensuring its inheritance (van Dooren *et al.*, 2005). After overnight incubation to generate a greater number of mature parasites, we identified similar apicoplast forms between WT and KO parasites in the mixed blood stage parasite population. Immunofluorescence assays with apicoplast-specific anti-ACP antibodies revealed no evident difference in the morphology of this organelle between WT and *LipB*-deficient asexual blood stage parasites (Fig. 2C; Fig. S1).

Parasites lacking *PbLipB* show reduced lipoylation of apicoplast and mitochondrial α -ketoacid dehydrogenases

We determined the effect of *PbLipB* deletion on parasite protein lipoylation by Western blot analysis using lipoic acid-specific antibodies. Results showed markedly reduced levels of lipoylated PDH-E2 (estimated at 84% reduction) in the *LipB*-deficient parasites compared to the WT control (Fig. 2D). This result is consistent with the proposal that *LipB* lipoylates PDH-E2 within the apicoplast (Gunther *et al.*, 2007). We note that *PbLipB* contains an apicoplast-targeting motif as predicted by PlasmoAP (Foth *et al.*, 2003) and PDH-E2 is the only protein within the apicoplast that is known to require lipoylation (Foth *et al.*, 2005). The other three proteins known to be lipoylated in *Plasmodium* are BCDH-E2, KGDH-E2, and the H-protein, which appear to localize to the mitochondria based on GFP-fusion studies in *P. falciparum* (Gunther *et al.*, 2005; Spalding *et al.*, 2010a). These proteins were predicted to be lipoylated by the mitochondrial ligases LplA1 or LplA2 (Wrenger *et al.*, 2004). Surprisingly, we found a substantial reduction in lipoylation of the BCDH-E2 protein (estimated at 98% reduction from overexposed Western blot images) in the *Pb LipB*

parasites compared to WT (Fig. 2D), suggesting that LipB also contributes to BCDH-E2 lipoylation in *P. berghei*. In contrast, KGDH-E2 lipoylation levels appeared unaffected by the loss of LipB. We note that this assay did not detect lipoylated forms of the 26 kDa H-protein, which is known to be difficult to detect because of its low abundance (Allary *et al.*, 2007).

Given the reduced degree of lipoylation of BCDH-E2 in Pb LipB parasites, we sought to investigate whether this protein might also localize to the apicoplast. This was tested by generating a *P. berghei* line in which *gfp* was integrated into the 3' end of the coding sequence of the *bcdh* gene, using *Tgdhfr-ts* as a selectable marker for homologous recombination and single site crossover. Live-cell imaging of BCDH-E2-GFP parasites stained with MitoTracker Red localized this fusion protein to the mitochondria (Fig. 2E). In contrast, BCDH-E2-GFP did not colocalize with the apicoplast, which was visualized using anti-ACP antibodies (Fig. 2F). These findings suggest that LipB might be responsible for the lipoylation of the mitochondrial protein BCDH-E2, and evoke the possible movement of lipoic acid from the apicoplast to the mitochondria. An alternative explanation would be that LipB, which has a N-terminal bipartite peptide that is predicted to traffic this protein to the apicoplast, could in part also traffic to the mitochondria. Experiments are underway to localize LipB by either GFP tagging or the use of polyclonal antisera.

Inhibition of lipoic acid scavenging with 8-BOA results in a decrease in asexual blood stage replication of Pb Δ LipB parasites

Our evidence suggesting that deleting the apicoplast-targeted octanoyl-ACP transferase may be impacting the lipoic acid supplied to the mitochondrial protein BCDH-E2 led us to test whether Pb LipB and WT parasites differed in their susceptibility to chemical inhibition of lipoic acid scavenging. For this we used the lipoic acid analog 8-BOA that is known to competitively inhibit the ligation of scavenged lipoic acid to its target α -ketoacid dehydrogenases within the mitochondria (Morris *et al.*, 1994; Allary *et al.*, 2007). 8-BOA is attached to enzymatic complexes by the scavenge pathway machinery; LplA1 protein attaches the antimetabolite in place of lipoic acid, rendering the complex metabolically inactive. 8-BOA inhibits the growth of *P. falciparum* asexual blood stage parasites by 70% at \sim 100 μ M after 96 hr of parasite exposure (Allary *et al.*, 2007) implying that scavenging of host lipoic acid is important for parasite blood stage proliferation. To assess the effect of short-term 8-BOA treatment on *P. berghei* replication, we collected WT and Pb LipB parasites from infected mice, and cultured these *in vitro* for 15 hr in the presence of 8-BOA (at concentrations of 100, 200 or 400 μ M). Parasites were then reinjected into naive mice (10,000 per mouse) to determine blood stage growth kinetics, without any further 8-BOA treatment. Experiments were performed on three independent occasions with five mice per group per experiment and parasitemias monitored daily once the infections became patent. We note that the asexual blood stage cycle of *P. berghei* is 24 hr.

Treatment of WT parasites with 8-BOA resulted in a modest reduction in parasitemia that generally attained statistical significance only at the highest inhibitor concentration (400 μ M) and only in the first three days following the onset of patent infections (Fig. 3A). In comparison, 8-BOA treatment showed a greater effect against LipB-deficient parasites, which showed significant decreases in parasitemia compared to DMSO-treated controls at the two higher concentrations for each day of monitoring (Fig. 3B). One explanation for these different blood stage growth kinetics of WT and LipB-deficient parasites treated with 8-BOA would be that apicoplast-generated lipoic acid might provide an important supplement for parasite growth. Specifically, synthesized lipoic acid might function to outcompete the 8-BOA present in the cell and the loss of *de novo* lipoic acid synthesis would shift the balance towards 8-BOA, generating a greater impact on parasite replication. These results suggest that the loss of LipB in the apicoplast is impacting the level of lipoic

acid throughout the parasite, allowing mitochondrial enzymes to be more susceptible to inactivation by conjugation with the antimetabolite. Alternatively, KO parasites might contain relatively less BCDH-E2 protein, although our RT-PCR analyses revealed similar levels of BCDH-E2 transcripts between WT and KO lines (data not shown). There also remains the possibility that LipB is partially localized within the mitochondria, despite its evident apicoplast-targeting motif.

PbΔLipB parasites demonstrate reduced blood stage growth rates upon reduction of host serum lipid concentrations

To test whether perturbation of host lipid levels would exacerbate the effect of *PbLipB* deletion and potentially reveal a blood stage phenotype, we lowered the levels of circulating lipids through the use of clofibrate. This prescription medicine activates the peroxisome proliferator-activated receptor- α in the liver, thereby inducing peroxisome biogenesis. This activation results in increased beta-oxidation of lipids and lowers the levels of cholesterol, triglycerides and non-esterified fatty acids (NEFA) circulating in the serum (Fruchart *et al.*, 1999; Wheelock *et al.*, 2007).

We treated mice daily for 9 days with 0, 0.5 or 5.0 mg/kg clofibrate, administered intraperitoneally. Mice were then rested for five days and the plasma was sampled to measure triglyceride and NEFA levels. Five mice were tested per group and the experiment was performed on three independent occasions. NEFA values in the three separate experiments were reduced by an average of $21.3 \pm 6.3\%$ and $37.2 \pm 17.9\%$ (mean \pm SD) in mice treated with 0.5 mg/kg and 5.0 mg/kg clofibrate respectively. Triglyceride values were only measured in the two latter experiments and were reduced by an average of $19.8 \pm 4.6\%$ and $27.8 \pm 5.3\%$ (mean \pm SD) in the 0.5 mg/kg and 5.0 mg/kg groups respectively. These results confirm the lipid-lowering properties of clofibrate.

Five days following the cessation of clofibrate treatment (i.e. the day of plasma sampling), mice were inoculated with 10,000 blood stage parasites and parasitemias were monitored daily by blood smear. We observed a statistically significant, dose-dependent reduction in the rate of blood stage parasite growth among WT parasites in treated mice for each day of monitoring (Fig. 3C). This effect was noticeably greater with the KO parasites, exemplified by the lack of detectable parasitemias by day seven in clofibrate-treated mice as compared to a mean parasitemia of 7% in DMSO-treated controls (Fig. 3D). This significant reduction was maintained in subsequent days.

To test whether clofibrate treatment might have affected reticulocyte numbers, and skewed the rate of growth of reticulocyte-tropic parasites, we repeated the clofibrate dosing regimen with once-daily dosing for nine days, and sampled whole blood via tail vein collection on days 0, 3, 6, 9 and 14. Reticulocyte densities were measured by labeling cells with antibodies specific to the reticulocyte surface marker CD71 and the erythroid cell surface marker Ter119, and counting cells by flow cytometry. Results showed no significant impact of clofibrate on reticulocyte densities, which ranged from an average of 1.6% to 2.1% over time in mice administered clofibrate (0.5 or 5.0 mg/kg daily) or DMSO vehicle as a control (12 mice per group; Table S2). These data are consistent with clofibrate exerting an effect on LipB-deficient parasites as a result of its lipid-lowering properties.

Taken together, our 8-BOA and clofibrate results provide evidence that *P. berghei* parasites utilize circulating host lipids during blood stage growth and that lipid depletion impacts parasite growth. These data suggest that the LipB-deficient parasites are more dependent on scavenging host lipid species, and support the hypothesis that the apicoplast lipoic acid *de novo* synthesis pathway provides an important substrate for asexual blood stage growth in conditions where host lipids are limited.

PbΔLipB parasites do not demonstrate a discernible phenotype during mosquito stage development

Prior investigations into the effect of *LipB* disruption on *P. falciparum* assessed only asexual blood stage growth (Gunther *et al.*, 2007). To assess whether disruption of the *LipB* gene had any major impact on the mosquito stages of *Plasmodium*, we fed mosquitoes on mice infected with WT or Pb LipB parasites, dissected salivary glands and viewed midguts for the presence of oocysts on day 21 post blood-meal by phase-contrast microscopy. This experiment was performed on three separate occasions, and sporozoite numbers were calculated from groups of 5 to 20 mosquitoes per parasite strain. We observed mean \pm SD sporozoite loads of $15,313 \pm 8,055$ and $13,611 \pm 6,286$ for the WT and KO respectively. These assays indicate that the loss of LipB did not noticeably impair parasite development in the *Anopheles* mosquito vector, and provide evidence that normal levels of lipoylated protein are not required for *P. berghei* development within the mosquito host.

PbΔLipB pre-erythrocytic stage parasites display reduced infectivity in vivo

To test whether disruption of *LipB* impacted the progression of *Plasmodium* sporozoites through the liver, we inoculated mice with KO or WT sporozoites, and measured the pre-patent periods. For these experiments we used female C57BL/6 mice, which are highly susceptible to *P. berghei* infections (Scheller *et al.*, 1994; Yu *et al.*, 2008). The pre-patent period, defined as the number of days until detection of parasites in the blood stream, demonstrates the ability of sporozoites to establish infection and complete liver stage development in the mammalian host. Sporozoites were dissected from salivary glands of infected mosquitoes and injected by intravenous injection into C57BL/6 mice. Using inocula of either 10,000 or 1,000 sporozoites, we consistently saw a delay in the pre-patent period with the Pb LipB sporozoites (Table 1). Only 2 of 9 mice developed a blood stage infection following inoculation with 1,000 Pb LipB sporozoites, as compared to all mice becoming infected with the same dose of WT sporozoites. Furthermore, the mice that became infected with the KO parasites showed a 4-day delay in the pre-patent period compared to those infected with WT parasites. At an inoculum of 10,000 sporozoites, all mice infected with the Pb LipB strain developed a blood stage infection, but with a marked increase in the pre-patent period (from an average of 3.0 days with the WT strain to 7.6 days with the KO strain). It has been stated in the literature that a one-day delay in patency roughly signifies a 10-fold decrease in sporozoite infectivity (Gantt *et al.*, 1998). Overall, these data suggest that *PbLipB* is important for normal liver stage development in *P. berghei*. In light of our findings, we suggest that the ability of some LipB-deficient parasites to progress through to asexual blood stage infection is made possible by the residual lipoylation of PDH-E2 that maintains sufficient PDH functionality for some KO parasites to complete their liver stage development, albeit for less efficiently than with WT parasites.

Treatment of PbLipB-deficient parasites with the scavenging inhibitor 8-BOA confirms the dual contribution of the lipoic acid synthesis and scavenging pathways during liver stage development

We used 8-BOA to deplete protein lipoylation coming from the scavenging pathway active in the mitochondria (Allary *et al.*, 2007; Deschermeier *et al.*, 2012) and examined whether treated liver stage parasites displayed any residual lipoylation that was attributable to apicoplast-synthesized lipoic acid. Developing parasites were treated with this competitive inhibitor and stained at 48 hr post invasion (hpi) with lipoic acid-specific antibodies, which can detect lipoylated proteins within the parasite and in the host hepatocyte (Fig. 4). For the WT control, we used a *P. berghei* ANKA line that expresses mCherry in the parasite mitochondria (Graewe *et al.*, 2009). In the case of the KO parasites, MitoTracker Red was used to label the mitochondria (both of the parasite and the host cell). Representative parasite images are shown in Fig. 4, with additional parasites shown in Fig. S2. WT

parasites (treated with DMSO vehicle) showed lipoic acid staining both within the parasite mitochondria (see colocalization of green lipoic acid and red mitochondrial signals in top row of Fig. 4A), as well as outside the parasite in the host cell (see green signal external to the parasite boundaries). Treatment with 8-BOA led to reduced lipoic acid staining in the parasite mitochondria, as expected (second row, Fig. 4A). Lipoylated proteins were nonetheless observed in the host hepatocyte, likely because the rate of protein turnover is slower and because the host mitochondria primarily rely on lipoic acid synthesis (Yi and Maeda, 2005), making them less affected by the addition of 8-BOA. With LipB-deficient parasites (treated with DMSO), we saw colocalization of lipoic acid and the mitochondria in the parasite (as well as in the host cell; see top row in Fig. 4B). Treatment with 8-BOA led to a marked loss of lipoic acid staining in the parasite mitochondria (see bottom row, Fig. 4B).

To quantify this analysis, we developed a program to measure the intensity of lipoic acid staining in multiple WT and KO liver stage parasites. Results, expressed as signal intensity per μm^2 of parasite, showed a significant decrease in the amount of lipoylated proteins in both WT and KO parasites following 8-BOA treatment, as compared to DMSO controls (estimated at 40% and 54% respectively; Fig. 4C). When compared to WT parasites, KO parasites also showed a significantly reduced amount of protein lipoylation following 8-BOA treatment (estimated at 68%; Fig. 4C). These data confirm that without scavenging of exogenous lipoic acid, only minimal lipoylated protein remained within the confines of LipB-deficient parasites.

To extend these observations, we examined lipoylated proteins within the apicoplasts of liver stage parasites at 48 hpi by performing a sequential staining procedure with anti-lipoic acid and anti-ACP antibodies. When merging these images, the majority of apicoplast structures colocalized with lipoylated proteins in WT parasites. However, significant portions of the apicoplast organelle were not lipoylated in KO parasites (example provided in Fig. S3). These preliminary data are consistent with our Western blot results showing reduced lipoylation of the apicoplast PDH-E2 subunit in LipB-deficient liver stage parasites (Fig. 2D).

Pb Δ LipB parasite apicoplast appears smaller and more constricted during the liver stage of development

Given that *LipB* is an apicoplast-targeted protein, we decided to examine the overall morphology of apicoplast development during the liver stage. WT and Pb LipB parasites were stained with antibodies to the apicoplast marker ACP as well as other antibodies that enabled us to measure the surface area of the developing parasite. These antibodies were specific to the Circumsporozoite Protein (CSP), Exported Protein-1 (EXP-1), or Merozoite Surface Protein-1 (MSP-1). CSP is expressed on the sporozoite surface (Ejigiri and Sinnis, 2009) and was used to identify the morphology of the young intra-hepatic parasite at 6 hpi. *P. berghei* EXP-1 is inserted into the parasitophorous vacuole membrane (PVM) that separates the replicating parasites from the host hepatocyte (Simmons *et al.*, 1987) and was used to measure the confines of the PVM. MSP-1 is a glycosylphosphatidylinositol (GPI)-anchored surface protein that peaks in expression at ~50 hpi in WT liver stage parasites (corresponding to late schizogony and the early cytomere stage) (Combe *et al.*, 2009). This protein becomes integrated into the parasite plasma membrane (PPM) and mediates attachment of merozoites to the surface of red blood cells (Cowman and Crabb, 2006). Mature hepatic merozoites express abundant amounts of MSP-1 on their surface, similar to the asexual blood stage counterparts. Antibodies to MSP-1 were used to determine the morphology of the PPM of late liver stages (schizonts, cytomeres and mature infectious merozoites) (Stanway *et al.*, 2009). Fluorescence imaging revealed no evident difference between WT and Pb LipB KO liver stage parasites at 6 and 24 hpi (see example in Fig.

5A). However, at later time points (48 hr and 54 hpi) we observed fewer branched structures in KO parasites. To quantify this, we measured the intensity of labeling with antibodies to the apicoplast marker ACP, for 12 to 18 parasites per strain and per time point. This MATLAB-based analysis showed a statistically significant, 65 to 67% reduction in total apicoplast surface area in KO compared to WT parasites (Fig. 5B). Exemplar parasite images are shown in Fig. 5A and additional parasites examined at 48 and 54 hpi are represented in Figs. S4 and S5 respectively. These findings contrast with the lack of observable differences between the apicoplasts of WT and LipB KO asexual blood stage parasites, and suggest that the deletion of *PbLipB* impacted the morphology of this organelle late in liver stage maturation.

We also counted the number of ACP-positive branch points reaching into the periphery of the developing parasite and contacting the MSP-1 labeled PPM for 40 parasites per time point, divided equally between WT and KO cultures. WT parasites yielded 7.4 ± 5.8 and 13.1 ± 4.3 (mean \pm SD) “contact points” between branches of the apicoplast and the PPM, at 48 and 54 hpi, respectively. In comparison, KO parasites had an average of 4.4 ± 3.6 and 3.9 ± 2.1 contact points at 48 and 54 hpi (the latter time point was significantly different between the WT and KO lines; $P < 0.0001$ based on Mann-Whitney U test). These data further suggest impaired apicoplast development in the KO line as it progresses to the late liver stage.

Pb Δ LipB parasites have major defects during late liver stage development and do not produce detached cells during in vitro culture

To further probe the defect in liver stage development in Pb LipB parasites, we generated a new *Pb LipB* KO parasite in the *P. berghei* ANKA GFP-Luciferase background, which expresses GFP-Luciferase from the strong *ef-1* promoter active throughout the parasite life cycle (Janse *et al.*, 2006a). We used Pb LipB-GFP-Luciferase and control GFP-Luciferase sporozoites to infect HepG2 cells. At 48 hpi, we determined the size of the exo-erythrocytic forms. The area of the developing parasites, as identified by measuring the area of the fluorescence emitted from the GFP-positive parasites, was found to not differ significantly between the two parasite lines (Fig. 6A). Nevertheless, quantitative RT-PCR studies with RNA harvested 48 hpi revealed a 10 to 12 fold reduction in *msp-1* transcript levels in the KO parasites compared to WT parasites, as determined using the $2^{-C(t)}$ method (Price *et al.*, 2004) with actin as an internal control (data not shown).

To further test for defects in liver stage development, we determined the total number of infected cells at several time points of liver stage development, using our Pb LipB parasites. From three independent experiments we identified no significant difference between the absolute number of developing parasites at 24 and 48 hpi (Fig. 6B), confirming our earlier results that the KO parasites initially develop normally. At 65 hpi (data not shown) and 84 hpi (Fig. 6B), the numbers of infected HepG2 cells with WT parasites began to decrease, as cells containing mature merozoites detached from the adherent surface. Approximately 20 to 30% of WT ANKA parasites were capable of successfully completing *in vitro* liver stage development, resulting in the detachment of the infected hepatocytes from the culture surface. These detached cells floating in the culture supernatant were quantified at 65 hpi, showing a clear contrast between the presence of detached cells in the WT cultures and their absence in the KO (Fig. 6B). These data suggest a defect in the maturation of late liver stage parasites in LipB-deficient parasites.

To more precisely define the stage of developmental arrest of LipB liver stage parasites, we performed immunofluorescence assays with cultured KO and WT parasites at 54 hpi and beyond. MSP-1 elucidated the morphology of the parasite plasma membrane (PPM), which at late time points invaginates around the individual daughter merozoites (Sturm *et al.*,

2009). WT ANKA parasites had well segregated individual nuclei by 54 hpi, with PPMs that evenly surrounded the developing clumps of merozoites (Fig. 6C, left panel; additional WT and KO images provided in Fig. S6 and S7). At similar or later time points, Pb LipB parasites demonstrated uneven MSP-1 staining that appeared to clump and not uniformly surround the daughter cells (Fig. 6C; see the representative 62 hr cytomere stage in the right panel). Rarely, we observed Pb LipB-infected cells containing what appeared to be morphologically normal merozoites. These parasites, however, were only seen at ~84 hpi, in comparison to the normal timeframe of 65 hpi required for complete *in vitro* development of WT parasites. The abnormal MSP-1 staining in the Pb LipB parasites suggests that the PPMs improperly segregating late in development, and suggests a key requirement for lipoic acid synthesis for successful intra-hepatic parasite maturation.

DISCUSSION

Here, we show that *P. berghei* sporozoites lacking the octanoyl-ACP transferase enzyme LipB have a profound loss of infectivity for the rodent host, caused by a defect in liver stage parasite development. These data argue for the importance of lipoylation to sustain the functionality of the α -ketoacid dehydrogenases PDH and BCDH during this phase of prodigious replication. These multi-enzyme complexes contribute to the FAS-II pathway (in the case of PDH) and the tricarboxylic acid (TCA) cycle (for BCDH). In contrast to the late liver stage arrest, LipB-deficient *P. berghei* parasites progressed unimpeded through their asexual blood stage cycle under standard *in vitro* or *in vivo* conditions, where the scavenging pathway is thought to supply most of the lipoic acid requirements. Nonetheless, chemical inhibition of the scavenging pathway using the lipoic acid analog 8-BOA, or lowering of host lipid levels by clofibrate treatment, provides evidence for an important contribution of the synthesis pathway in asexual blood stage parasites in lipid-limiting host environments.

A striking feature of these LipB-deficient parasites was the late stage at which intra-hepatic arrest occurred. Immunofluorescence assays with Pb LipB parasites showed the presence of the merozoite surface marker MSP-1, indicating progression through to the cytomere stage that precedes the final phase of maturation. However, MSP-1 labeling appeared abnormal, and *in vitro* we could not detect detached cells. These cells are indicative of the mature merosomes that are enveloped by host hepatocyte membrane and that contain merozoites that can invade erythrocytes (Prudencio *et al.*, 2006; Rankin *et al.*, 2010). In comparison, *P. berghei* or *P. yoelii* parasites lacking FAS-II enzymes typically arrested prior to MSP-1 expression, as did the *P. yoelii* KO parasites lacking PDH-E1 or PDH-E3 (Yu *et al.*, 2008; Vaughan *et al.*, 2009; Pei *et al.*, 2010; Annoura *et al.*, 2012). Indeed, the LipB KO arrest occurred later than any of the genetically attenuated parasites reported to date (Mueller *et al.*, 2005a; Mueller *et al.*, 2005b; van Dijk *et al.*, 2005; Khan *et al.*, 2012). This is of particular interest for the development of genetically attenuated vaccines, as recent evidence indicates that mature liver stages are a superior immunogen to early stages in terms of eliciting robust, durable protective immunity (Friesen *et al.*, 2010; Borrmann and Matuschewski, 2011; Butler *et al.*, 2011). Clearly, the LipB KO would not suffice, as we observed breakthrough infections in the sensitive *P. berghei* ANKA – C57BL/6 mouse model (Annoura *et al.*, 2012), and additional layers of attenuation would be required. One candidate could be LplA2, a lipoate ligase that is targeted to both the apicoplast and the mitochondria and that has been proposed to mediate partial PDH-E2 lipoylation in LipB-deficient *P. falciparum* parasites (Gunther *et al.*, 2007).

To probe the biological basis of why LipB-deficient parasites arrest later than their FAS-II or PDH counterparts during liver stage development, one must consider the different roles of these related pathways. Our data suggest that LipB is important for maintaining normal

levels of lipoylation of the α -ketoacid dehydrogenases PDH and BCDH in *P. berghei*. Without a lipoylated E2 subunit, dehydrogenases are catalytically inactive (Perham, 2000). In most eukaryotic cells, PDH transforms pyruvate into acetyl-CoA for the generation of TCA intermediates for cellular respiration and glycolysis (Dumollard *et al.*, 2009). However, *Plasmodium* encodes only a single PDH that is targeted to the apicoplast, where its likely role is to provide acetyl-CoA for the FAS-II pathway (Foth *et al.*, 2005; Pei *et al.*, 2010). PDH-E2 lipoylation requires octanoyl-ACP produced by FAS-II; hence the enzymatic activity of PDH is tightly regulated because of the interdependence between these pathways. One interpretation of our findings is that the LipB KO liver stage arrest is simply due to reduced lipoylation of PDH-E2 that can no longer functionally generate acetyl-CoA for FAS-II. The fact that the LipB KO parasites still have a residual amount of lipoylated PDH-E2 protein might explain why these parasites continue developing very late during liver stage, and arrest later as compared to the PDH or FAS-II KO parasites. Another explanation would involve BCDH, whose E2 subunit was observed to be substantially less lipoylated in blood stage parasites. In eukaryotic cells, BCDH degrades the branched chain amino acids valine, leucine and isoleucine, presumably for the generation of acetyl-CoA or succinyl-CoA intermediates for the TCA cycle (Gunther *et al.*, 2005). Intermediates of this cycle have been isolated from *P. falciparum* blood stage parasites, which use glutamate and glutamine as major carbon sources (Olszewski *et al.*, 2010). The importance of the TCA cycle in liver stages remains to be clarified. Intriguingly, transcriptional profiling by microarrays has revealed up-regulation of other TCA-related genes, including components of the BCDH complex, in intra-hepatic parasites (Tarun *et al.*, 2008). Therefore, the importance of LipB during liver stage development could involve both the FAS-II and the TCA cycles that depend on acetyl-CoA. A third possibility could relate to the known role of lipoic acid as an antioxidant (Goraca *et al.*, 2011; Packer and Cadenas, 2011). This property is related to the ability of oxidized lipoate and its reduced form, dihydrolipoate, to form a redox couple that can effectively quench reactive oxygen species (including hydroxyl, peroxy and superoxide radicals), as well as interact with other antioxidants including glutathione, vitamins C and E and coenzyme Q (Spalding *et al.*, 2010b). While much has yet to be elucidated about whether *Plasmodium*-infected hepatocytes generate oxidative stress that can impede intracellular parasite development, indirect evidence comes from the observation that parasitized hepatocytes upregulate host cell redox pathways (Albuquerque *et al.*, 2009; Dey *et al.*, 2009). It is tempting to speculate that *Plasmodium* may require the antioxidant properties of lipoic acid to protect itself against hepatocyte defense mechanisms. Redox-perturbing agents would be useful for future studies to test this hypothesis.

One intriguing finding from our study was the reduced lipoylation of BCDH-E2 in our LipB-deficient *P. berghei* asexual blood stage parasites. Similar results were obtained with *P. falciparum* LipB KO parasites that showed reduced lipoylation of BCDH-E2 and PDH-E2 but not KGDH-E2 (Gunther *et al.*, 2007). These data suggest that apicoplast-derived lipoic acid can be delivered to the mitochondria, a scenario that differs from the current working models in *Plasmodium* and *Toxoplasma gondii* that the mitochondrial α -ketoacid dehydrogenases are only modified with lipoic acid scavenged from the host (Allary *et al.*, 2007). In preliminary Western blot studies with our *P. berghei* parasites incubated \pm 8-BOA (tested at 400 μ M), we found minor (13–41%) reductions in lipoylation of apicoplast and mitochondrial dehydrogenases in KO parasites, contrasting with zero reduction of lipoylation in WT parasites (unpublished observations). In *P. falciparum*, the effects of 400 μ M 8-BOA are readily reversed by only 2 μ M of additional lipoic acid (Allary *et al.* 2007). Human serum is known to typically contain 160–700 nM lipoic acid (Storm and Muller, 2012), however we could not find any literature on rodents. While further studies are required to control for exogenous lipoic acid in these assays, these results are consistent with LipB contributing to lipoylation of mitochondrial BCDH-E2 (Fig. 2D). These findings also support other data suggesting that the reduction of *de novo* lipoic acid results in the parasite

becoming more dependent on the scavenge pathway and hence more susceptible to the scavenge inhibitor, 8-BOA.

We also propose that liver stage development requires both active lipoic acid synthesis and its import into the mitochondria. This proposal is based on the liver stage arrest phenotype that we observed with LipB-deficient parasites as well as earlier reports of liver stage inhibition with the lipoic acid analog 8-BOA that inactivates mitochondrial α -ketoacid dehydrogenases (Allary *et al.*, 2007; Deschermeier *et al.*, 2012). This differs from asexual blood stage parasites where disruption of the apicoplast FAS-enzymes, the PDH complex or, in the present study LipB, does not impede parasite development that appears to depend primarily on parasite pathways to import host fatty acids or lipoic acid. Of note, a recent study in *P. falciparum* implicated isoprenoid synthesis as the sole apicoplast pathway required for asexual blood stage development. (Yeh and DeRisi, 2011). This pathway produces isopentenyl pyrophosphate, which is used to synthesize isoprenoids whose uses include post-translational protein modifications (Nguyen *et al.*, 2010). Available evidence suggests that, compared to the asexual blood stages, liver stage parasites are much more dependent on apicoplast de novo biosynthetic pathways, including for the production of lipoic and fatty acids (Yu *et al.*, 2008; Vaughan *et al.*, 2009; Pei *et al.*, 2010; Annoura *et al.*, 2012).

While arrested in their maturation in hepatocytes, no developmental or growth defect was observed with LipB KO parasites during their asexual blood stage replication. These findings are similar to the published reports with the FAS-II and PDH KO lines (Yu *et al.*, 2008; Vaughan *et al.*, 2009; Pei *et al.*, 2010). In the case of the FAS-II KOs, this has been attributed to fatty acid salvaging being sufficient for asexual blood stage replication and growth, which would also explain the lack of a requirement for the PDH product acetyl-CoA that primes the FAS-II pathway. Interestingly, our study detected an effect of the LipB KO in conditions where host lipid levels were perturbed. Using the lipoic acid analog 8-BOA that competitively inhibits lipoic acid attachment in the mitochondria (Allary *et al.*, 2007), we found significantly reduced rates of asexual blood stage growth in the synthesis-deficient KO line. Less pronounced inhibition was observed with WT parasites. These data are consistent with parasites having a mechanism to import lipoic acid into their mitochondria, and suggest that this import pathway is even more critical when parasites can no longer furnish their own source of lipoate.

Our findings suggest that LipB plays an active role in asexual blood stage parasites and might become critical for parasite proliferation in cases where insufficient lipoic acid can be scavenged from the host plasma. This conclusion is further supported by the findings *in vivo* by reducing the circulating lipid levels of mice with clofibrate treatment. Under these conditions, the LipB-deficient parasites showed a substantially greater attenuation of blood stage growth compared to the WT control strain, suggesting a need for lipoylated PDH to support FAS-II activity in lipid-deprived conditions. This could be especially relevant in malnourished individuals with very low levels of circulating lipids. While we could not identify any published reports of lipoic acid levels in African children, there is abundant literature on the prevalence of moderately or severely acute malnutrition in young African children, who bear the brunt of malarial disease (Victoria *et al.*, 2008; LaGrone *et al.*, 2012). We conjecture that parasite pathways such as lipoic acid or fatty acid synthesis, which are apparently not required for asexual blood stage proliferation *in vitro*, might be important pathways that *P. falciparum* can exploit to sustain rapid growth in malnourished individuals.

Recent years have seen an increasing focus on how *Plasmodium* co-opts host metabolites for its benefit and how this parasite balances scavenging pathways with the need for supplementation via *de novo* synthesis, as it progresses through its life cycle. Deciphering

the key molecular determinants and their stage specificity should expose weaknesses that can be exploited to develop genetically attenuated parasite vaccines or chemotherapeutic agents designed to prevent or cure disease. *Plasmodium* clearly exploits human metabolism, and one suspects that this includes the use of pathways that sustain growth in instances of human malnutrition. A core challenge will be to develop ways to intervene in these pathways to cure infections and reduce the burden of disease.

EXPERIMENTAL PROCEDURES

Propagation of *P. berghei* parasites

P. berghei ANKA (MRA-671) parasites were passaged via intraperitoneal injection in female Swiss-Webster or NMRI mice and pre-patent periods were determined in female C57BL/6 mice (6–8 weeks old at the time of experimentation; Taconic). Parasitized mice were euthanized at the first signs of distress. Animal experimentation performed at Columbia University or the Bernhard-Nocht-Institute complied with protocols and regulations approved by the Institutional Animal Care and Use Committee of Columbia University or the ethical committee of Hamburg State authorities.

Plasmid constructs and parasite transfections

To delete *PbLipB* (PlasmoDB ID: PBANKA_070700), we first constructed the plasmid pL0001-*PbLipB*, containing 5' and 3' UTRs specific to this genomic locus. These 0.68 kb and 0.85 kb products (respectively) were PCR amplified from *P. berghei* ANKA genomic DNA using primers P2268 + P2269, and P2182 + P2350 (Table S1). Fragments were subcloned between the EcoRV / XbaI and Acc65I / HindIII sites of pL0001 (de Koning-Ward *et al.*, 2000). The final plasmid was linearized by XbaI, ScaI and Acc65I digestion and verified by agarose gel electrophoresis prior to transfection. Electroporation and selection with pyrimethamine (0.07 mg/ml in the drinking water) was performed as previously described (Carvalho and Menard, 2005; Janse *et al.*, 2006b). *Pb LipB* KO clones were obtained by limited dilution in mice. Homologous recombination leading to deletion of the endogenous *PbLipB* coding sequence and its replacement by the *T. gondii dhfr-ts* marker (Donald and Roos, 1993) was confirmed by PCR (see Fig. 1), using the following primers: P2302 (p1) + P2303 (p2), P2448 (p3) + P2344 (p4), P2343 (p5) + P2453 (p6), P2320 (p7) + P2448, P2453 + P2317 (p8), P2345 (p9) + P2346 (p10).

To localize BCDH, we generated the plasmid pL0031-BCDH-GFP. For this, 875 bp of the 3' end of *bcdh-E2* (PlasmoDB ID: PBANKA_141110) coding sequence was PCR amplified from ANKA genomic DNA using the primers P2872 + P2873. The product was cloned between the SacII / NcoI sites in pL0031 (Kooij *et al.*, 2005) to create a *bcdh-gfp* fusion. This construct, containing the *T. gondii dhfr-ts* marker, was linearized with BsmBI prior to electroporation into *P. berghei* ANKA. Recombinant parasites were selected with pyrimethamine as described above. Correct integration into *bcdh-E2* following homologous recombination and single site crossover resulted in the introduction of *gfp* as a 3' fusion, and was confirmed by PCR using primers P2957 + P3053.

Kinetics of blood stage growth in *PbΔLipB* and wild-type ANKA parasites

Parasites were administered intravenously to Swiss-Webster mice and their parasitemias were monitored daily by microscopic examination of Giemsa-stained thin blood smears. Three independent experiments were performed; each comprising two groups of five mice infected with either *Pb LipB* or parental asexual blood stage WT parasites.

Immunofluorescence analysis of blood stage parasites

P. berghei ANKA, Pb LipB, or PbBCDH-E2-GFP asexual blood stage parasites were prepared for immunofluorescence following formaldehyde / glutaraldehyde fixation and Triton X-100 permeabilization, as described (Tonkin *et al.*, 2004). Cells were incubated with rabbit anti-ACP IgG (diluted 1:2000; (Waller *et al.*, 2000) followed by AlexaFluor 594 secondary anti-rabbit antibodies (diluted 1:1000; Molecular Probes). Cells were imaged in complete medium (Janse *et al.*, 2006b) containing Hoechst (5 µg/ml). PbBCDH-E2-GFP parasites were incubated with 20 nM MitoTracker Red CMXRos (Invitrogen) for 20 minutes at 37°C prior to fluorescence microscopy.

Western blot analysis of lipoylated proteins

Infected RBCs were collected from mice with 8–10% parasitemias and saponin-lysed prior to protein extraction in RIPA lysis buffer (Boston BioProducts) supplemented with protease inhibitors (Roche Applied Science). Samples were subjected to SDS-PAGE and the gels transferred onto nitrocellulose membranes. Membranes were incubated with rabbit polyclonal anti-lipoic acid IgG (diluted 1:1000; Calbiochem) followed by secondary anti-rabbit IgG conjugated to horseradish peroxidase (diluted 1:2500; GE Healthcare).

Treatment of asexual blood stage parasites with the lipoic acid analog 8-BOA

P. berghei-infected RBCs were incubated overnight 37°C in complete medium (Janse *et al.*, 2006b) containing 8-BOA (100 µM, 200 µM or 400 µM in 0.004% final DMSO) or a control solution of 0.004% DMSO. 10,000 infected RBCs were then inoculated into naïve mice by tail vein injection. Parasitemias were monitored by microscopic assessment of Giemsa-stained thin smears for 8 days.

P. berghei blood stage growth kinetics in clofibrate-treated mice

Uninfected Swiss-Webster mice were intraperitoneally administered 0.5 mg/kg or 5.0 mg/kg clofibrate or an equal volume (50 µl) of DMSO control, daily for 9 days. On days 5 and 9, tail vein blood (30 µl per mouse) was drawn. Plasma was separated by centrifugation and used in enzymatic-based colorimetric assays to determine the levels of circulating non-esterified fatty acids and triglycerides (HR Series NEFA-HR and L-Type TG M kits; WAKO Diagnostics). After the 9-day treatment, mice were inoculated with 10,000 infected RBCs and growth kinetics were monitored daily for an additional 9 days by thin-smear microscopy. To determine reticulocyte densities, groups of 12 Swiss-Webster mice each were administered 0.5 mg/kg or 5.0 mg/kg clofibrate or an equal volume (50 µl) of vehicle control, daily for 9 days as above. On days 0, 3, 6, 9 and 14 one microliter of blood was collected from each mouse into complete media containing citrate-phosphate-dextrose (Sigma) via slight nicking of the tail vein. After incubation with Fc receptor block (anti-CD16/CD32, Invitrogen), cells were stained with antibodies specific to the transferrin receptor CD71 (FITC Anti-CD71; BD Pharmingen) and Ter119 (PE Anti-Ter119; BD Pharmingen) (Posluszny *et al.*, 2011). Cells were subjected to flow cytometry on an Accuri C6 desktop cytometer, and at least 20,000 events were analyzed for each sample using FlowJo software.

Mosquito infections with *P. berghei*

Anopheles stephensi mosquitoes were fed on anesthetized Swiss-Webster or NMRI mice infected with Pb LipB or *P. berghei* ANKA parasites, and were maintained in incubators with 70–80% humidity set at 19°C at Columbia University or 21°C at the Bernhard-Nocht-Institute. Oocysts were examined in dissected midguts using phase-contrast microscopy.

In vivo liver stage development assays

Salivary glands from infected mosquitoes were dissected by hand on day 21-post blood meal and sporozoites were quantified using a hemocytometer. Sporozoites were inoculated into C57BL/6 mice using tail-vein injections. Pre-patent periods were determined by thin-smear microscopy.

In vitro liver stage assays

HepG2 cells (ATCC) were seeded in 24-well plates containing glass cover slips at 6×10^4 cells per well and cultured at 37°C. After 24 hr, salivary gland sporozoites were added ($2-3 \times 10^4$ per well). Two hr later, 200 μ M 8-BOA (or a DMSO vehicle control; final concentration 0.12%) was then added to deplete scavenged lipoic acid from liver stage parasites. Cells were then incubated in the presence of 8-BOA at 37°C in 5% CO₂ for 48 hr. Infected cells were then incubated with 250 nM MitoTracker Red CMXRos (Invitrogen) for 15 min and fixed/permeabilized with 4% paraformaldehyde and methanol. Primary antibody (rabbit anti-lipoic acid diluted 1:1000) was applied for 2 hr at room temperature in 10%FCS/PBS. Cells were washed three times with PBS and secondary antibodies (donkey anti-rabbit Fluor647 diluted 1:1000) and DAPI (1 μ g/ml) were applied in 10%FCS/PBS for 1 hr at room temperature. Microscopic analysis was done on a FluoView FV1000 confocal microscope.

To perform quantitative analysis of the lipoylated areas of liver stage parasites (Fig. 4C), we first defined the edges of the parasitophorous vacuoles using the Canny edge detection algorithm (Canny, 1986). Internal regions were then isolated without holes as a separate image and imported in Python. Cropped anti-lipoic acid images were analyzed in the MATLAB Image Analysis Toolbox (Mathworks, California) for total intensity (using 32 bit unsigned integer RGB data), total area of the parasite (in pixels) and total illuminated area of the parasite (in pixels) using the standard gray threshold generation function after conversion to a grayscale image. The ratio of the intensity to the proportional area illuminated was then reported for each parasite separately. Data were converted into intensity per micrometer-squared of parasite and the standard error was determined per group. Mann-Whitney U tests between parasite lines at each condition were used to determine statistical significance. This analysis was repeated to calculate the apicoplast surface area in KO vs. WT parasites (Fig. 5B), this time measuring the intensity of staining with anti-ACP instead of anti-lipoic acid antibodies.

In the sequential staining procedure with the -lipoic acid and -ACP antibodies, infected HepG2 cells were fixed and permeabilized with the same conditions as listed above. Cells were incubated with rabbit anti-lipoic acid (1:2,000 in 10% FCS/PBS) for 2 hr, washed three times with 1 \times PBS and incubated with goat anti-rabbit Hilyte647 (1:1,000 in 10% FCS/PBS) for 1 hr. Cells were washed three times with PBS. Following anti-lipoic acid staining, cells were incubated with goat anti-rabbit horseradish peroxidase (1:20 in 10% FCS/PBS) for 1 hr, washed three times with PBS and incubated with 10% rabbit serum / 1 \times PBS for 1hr. Cells were washed three times with PBS and then incubated with rabbit anti-ACP (1:500) and chicken anti-Exp-1 (1:2000) in 10% FCS/ PBS overnight at 4°C. Cells were washed again three times with PBS and incubated with goat anti-rabbit Alexa594 (1:5000), donkey anti-chicken Cy2 (1:250) and DAPI (final concentration 1 μ g/ml) in 10% FCS/PBS for 1 hr. All incubations were at room temperature. Cover slips were washed three times with PBS, dipped in H₂O and mounted on glass slides using Daco Fluorescent Mounting Medium prior to fluorescence microscopy imaging (Fig. S3).

To determine the morphology of the apicoplast, liver stage infections were established as above. At the indicated times, cell were fixed/permeabilized with 4% paraformaldehyde and

methanol and incubated with the primary antibodies at the time points indicated (mouse anti-CSP 1:1000; chicken anti-Exp-1 1:1000; mouse anti-MSP-1 1:2000; rabbit anti-ACP 1:1000) was applied for 2 hr. Secondary antibodies (anti-mouse Alexa 594 1:5000 plus anti-rabbit Hilyte 647 1:1000; or anti-chicken Alexa 594 1:5000 plus anti-rabbit Hilyte 647 1:1000) were applied for 1 hr. Images were captured on a FluoView™ FV1000 confocal microscope.

To assess the size of liver stage parasites, a *P. berghei* line that constitutively expresses GFP-Luciferase (Franke-Fayard *et al.*, 2004); MRA-868) was transfected with the pL0001-*PbLipB* plasmid and KO clones disrupted in the *LipB* locus were isolated as described above. Liver stage parasites were visualized by fluorescence microscopy and parasite size was analyzed from 150 to 200 cells per line (KO or parent) using ImageJ software.

To determine the absolute number of developing liver stage parasites, HepG2 cells were infected with 10⁴ WT or LipB KO sporozoites, respectively. Infected cells were fixed and permeabilized 24 and 48 hpi and were stained using either a mouse anti-RFP antibody (WT controls expressed cytosolic mCherry (Graewe *et al.*, 2009)) or rat antiserum raised against *P. berghei* blood stage parasites (used for *Pb LipB*). Parasites were counted using a Leitz-DM RB fluorescence microscope (Leica). At 65 hpi “detached cells” were stained with Hoechst 33342 and were counted using an Axiovert 200 fluorescence microscope (Zeiss). Immunofluorescence for developmental markers of liver stage parasites was completed with primary antibodies (chicken anti-Exp-1 1:1000, mouse anti-MSP 1:2000), which were applied for 2 hr at room temperature. Secondary antibodies (anti-chicken Cy2 1:250, anti-mouse Alexa 594 1:5000) and DAPI (1 µg/ml) were applied for 1 hr at room temperature. *In vitro* cultures were also used for the generation of parasite cDNA after 48 hrs of development.

For RT-PCR studies, we harvested infected HepG2 cells at 48 hpi, and purified the RNA from KO and WT parasites using Trizol and RNeasy kits (Qiagen). For RT-PCR assays we used a SuperScript III kit (Invitrogen) to generate cDNA and tested for transcription of *PbLipB* using primers p2304 (p1) + P2303 (p2) reactions ± reverse transcriptase (Fig. 1D). Control reactions included primers p3753 + p3754 specific for the *P. berghei* actin I gene (Angrisano *et al.*, 2012).

For q-RT-PCR assays, we purified mRNA using an Oligotex RNA isolation kit. Reactions were performed using two-fold dilutions of mRNA spanning the range of 4 to 128 ng mRNA, in a Bio-Rad Opticon 2 DNA Engine. Amplifications employed one-step iScript-RT-PCR kits (Bio-Rad) with SYBR Green, with the following conditions: 50°C for 30 min and 95°C for 15 min, followed by 40 cycles of 95°C for 30 s, 43°C for 30 s, 72°C for 30 s. Primers specific to *P. berghei msp-1* (PBANKA_08310) were: P3658 + P3659. Actin I (PBANKA_145930) was used as the internal reference, employing the primers p3753 + p3754. We also included reactions with a plasmid containing the *msp-1* target fragment to create a standard curve. *msp-1* transcript levels were determined relative to *actin* using the 2^{-C(t)} method (Price *et al.*, 2004).

Supplementary Material

Refer to Web version on PubMed Central for supplementary material.

Acknowledgments

We thank Drs. Andrea Ecker, Bamini Jayabalasingham, Eric Ekland, and Marcus Lee for their advice and help with the manuscript. *P. berghei* ANKA parasites (MRA-671, deposited by Mark Wiser; MRA-868, deposited by Chris Janse and Andy Waters), as well as the transfection plasmids pL0001 and pL0031 (MRA-770 and MRA-800, both

deposited by Andy Waters), were obtained through the MR4 (BEI Resources, Manassas, VA). Funding for this work was provided in part by the NIH (T-R01 AI095584, PI D. Fidock; R01 AI056840, PI P. Sinnis; and R01 AI065853, PI S. Prigge) and the EVIMaLaR EU-consortium (V. Heussler).

References

- Albuquerque SS, Carret C, Grosso AR, Tarun AS, Peng X, Kappe SH, et al. Host cell transcriptional profiling during malaria liver stage infection reveals a coordinated and sequential set of biological events. *BMC Genomics*. 2009; 10:270. [PubMed: 19534804]
- Allary M, Lu JZ, Zhu L, Prigge ST. Scavenging of the cofactor lipoate is essential for the survival of the malaria parasite *Plasmodium falciparum*. *Mol Microbiol*. 2007; 63:1331–1344. [PubMed: 17244193]
- Amino R, Thiberge S, Martin B, Celli S, Shorte S, Frischknecht F, Menard R. Quantitative imaging of *Plasmodium* transmission from mosquito to mammal. *Nat Med*. 2006; 12:220–224. [PubMed: 16429144]
- Angrisano F, Riglar DT, Sturm A, Volz JC, Delves MJ, Zuccala ES, et al. Spatial localisation of actin filaments across developmental stages of the malaria parasite. *PLoS One*. 2012; 7:e32188. [PubMed: 22389687]
- Annoura T, Ploemen IH, van Schaijk BC, Sajid M, Vos MW, van Gemert GJ, et al. Assessing the adequacy of attenuation of genetically modified malaria parasite vaccine candidates. *Vaccine*. 2012; 30:2662–2670. [PubMed: 22342550]
- Biewenga GP, Haenen GR, Bast A. The pharmacology of the antioxidant lipoic acid. *Gen Pharmacol*. 1997; 29:315–331. [PubMed: 9378235]
- Borrmann S, Matuschewski K. Targeting *Plasmodium* liver stages: better late than never. *Trends Mol Med*. 2011; 17:527–536. [PubMed: 21737347]
- Butler NS, Schmidt NW, Vaughan AM, Aly AS, Kappe SH, Harty JT. Superior antimalarial immunity after vaccination with late liver stage-arresting genetically attenuated parasites. *Cell Host Microbe*. 2011; 9:451–462. [PubMed: 21669394]
- Canny J. A computational approach to edge detection. *IEEE Trans Pattern Anal Mach Intell*. 1986; 8:679–698. [PubMed: 21869365]
- Carvalho TG, Menard R. Manipulating the *Plasmodium* genome. *Curr Issues Mol Biol*. 2005; 7:39–55. [PubMed: 15580779]
- Combe A, Giovannini D, Carvalho TG, Spath S, Boisson B, Loussert C, et al. Clonal conditional mutagenesis in malaria parasites. *Cell Host Microbe*. 2009; 5:386–396. [PubMed: 19380117]
- Cowman AF, Crabb BS. Invasion of red blood cells by malaria parasites. *Cell*. 2006; 124:755–766. [PubMed: 16497586]
- Crawford MJ, Thomsen-Zieger N, Ray M, Schachtner J, Roos DS, Seeber F. *Toxoplasma gondii* scavenges host-derived lipoic acid despite its *de novo* synthesis in the apicoplast. *EMBO J*. 2006; 25:3214–3222. [PubMed: 16778769]
- de Koning-Ward TF, Fidock DA, Thaty V, Menard R, van Spaendonk RM, Waters AP, Janse CJ. The selectable marker human dihydrofolate reductase enables sequential genetic manipulation of the *Plasmodium berghei* genome. *Mol Biochem Parasitol*. 2000; 106:199–212. [PubMed: 10699250]
- Deschermeier C, Hecht LS, Bach F, Rutzel K, Stanway RR, Nagel A, et al. Mitochondrial lipoic acid scavenging is essential for *Plasmodium berghei* liver stage development. *Cell Microbiol*. 2012; 14:416–430. [PubMed: 22128915]
- Dey S, Guha M, Alam A, Goyal M, Bindu S, Pal C, et al. Malarial infection develops mitochondrial pathology and mitochondrial oxidative stress to promote hepatocyte apoptosis. *Free Radic Biol Med*. 2009; 46:271–281. [PubMed: 19015023]
- Donald RG, Roos DS. Stable molecular transformation of *Toxoplasma gondii*: a selectable dihydrofolate reductase-thymidylate synthase marker based on drug-resistance mutations in malaria. *Proc Natl Acad Sci U S A*. 1993; 90:11703–11707. [PubMed: 8265612]
- Dumollard R, Carroll J, Duchon MR, Campbell K, Swann K. Mitochondrial function and redox state in mammalian embryos. *Semin Cell Dev Biol*. 2009; 20:346–353. [PubMed: 19530278]

- Ejigiri I, Sinnis P. *Plasmodium* sporozoite-host interactions from the dermis to the hepatocyte. *Curr Opin Microbiol.* 2009; 12:401–407. [PubMed: 19608456]
- Foth BJ, Ralph SA, Tonkin CJ, Struck NS, Fraunholz M, Roos DS, et al. Dissecting apicoplast targeting in the malaria parasite *Plasmodium falciparum*. *Science.* 2003; 299:705–708. [PubMed: 12560551]
- Foth BJ, Stimmler LM, Handman E, Crabb BS, Hodder AN, McFadden GI. The malaria parasite *Plasmodium falciparum* has only one pyruvate dehydrogenase complex, which is located in the apicoplast. *Mol Microbiol.* 2005; 55:39–53. [PubMed: 15612915]
- Franke-Fayard B, Trueman H, Ramesar J, Mendoza J, van der Keur M, van der Linden R, et al. A *Plasmodium berghei* reference line that constitutively expresses GFP at a high level throughout the complete life cycle. *Mol Biochem Parasitol.* 2004; 137:23–33. [PubMed: 15279948]
- Friesen J, Silvie O, Putrianti ED, Hafalla JC, Matuschewski K, Borrmann S. Natural immunization against malaria: causal prophylaxis with antibiotics. *Sci Transl Med.* 2010; 2:40ra49.
- Fruchart JC, Duriez P, Staels B. Molecular mechanism of action of the fibrates. *J Soc Biol.* 1999; 193:67–75. [PubMed: 10851558]
- Gantt SM, Myung JM, Briones MR, Li WD, Corey EJ, Omura S, et al. Proteasome inhibitors block development of *Plasmodium* spp. *Antimicrob Agents Chemother.* 1998; 42:2731–2738. [PubMed: 9756786]
- Goraca A, Huk-Kolega H, Piechota A, Kleniewska P, Ciejka E, Skibska B. Lipoic acid - biological activity and therapeutic potential. *Pharmacol Rep.* 2011; 63:849–858. [PubMed: 22001972]
- Graewe S, Retzlaff S, Struck N, Janse CJ, Heussler VT. Going live: a comparative analysis of the suitability of the RFP derivatives RedStar, mCherry and tdTomato for intravital and *in vitro* live imaging of *Plasmodium* parasites. *Biotechnol J.* 2009; 4:895–902. [PubMed: 19492329]
- Graewe S, Stanway RR, Rennenberg A, Heussler VT. Chronicle of a death foretold: *Plasmodium* liver stage parasites decide on the fate of the host cell. *FEMS Microbiol Rev.* 2012; 36:111–130. [PubMed: 22092244]
- Gunther S, McMillan PJ, Wallace LJ, Muller S. *Plasmodium falciparum* possesses organelle-specific alpha-keto acid dehydrogenase complexes and lipoylation pathways. *Biochem Soc Trans.* 2005; 33:977–980. [PubMed: 16246025]
- Gunther S, Wallace L, Patzewitz EM, McMillan PJ, Storm J, Wrenger C, et al. Apicoplast lipoic acid protein ligase B is not essential for *Plasmodium falciparum*. *PLoS Pathog.* 2007; 3:e189. [PubMed: 18069893]
- Gunther S, Storm J, Muller S. *Plasmodium falciparum*: organelle-specific acquisition of lipoic acid. *Int J Biochem Cell Biol.* 2009; 41:748–752. [PubMed: 19027872]
- Janse CJ, Franke-Fayard B, Mair GR, Ramesar J, Thiel C, Engelmann S, et al. High efficiency transfection of *Plasmodium berghei* facilitates novel selection procedures. *Mol Biochem Parasitol.* 2006a; 145:60–70. [PubMed: 16242190]
- Janse CJ, Ramesar J, Waters AP. High-efficiency transfection and drug selection of genetically transformed blood stages of the rodent malaria parasite *Plasmodium berghei*. *Nat Protoc.* 2006b; 1:346–356. [PubMed: 17406255]
- Khan SM, Janse CJ, Kappe SH, Mikolajczak SA. Genetic engineering of attenuated malaria parasites for vaccination. *Curr Opin Biotechnol.* 2012
- Kirk K, Saliba KJ. Targeting nutrient uptake mechanisms in *Plasmodium*. *Curr Drug Targets.* 2007; 8:75–88. [PubMed: 17266532]
- Kooij TW, Franke-Fayard B, Renz J, Kroeze H, van Dooren MW, Ramesar J, et al. *Plasmodium berghei* alpha-tubulin II: a role in both male gamete formation and asexual blood stages. *Mol Biochem Parasitol.* 2005; 144:16–26. [PubMed: 16115694]
- LaGrone LN, Trehan I, Meuli GJ, Wang RJ, Thakwalakwa C, Maleta K, Manary MJ. A novel fortified blended flour, corn-soy blend “plus-plus,” is not inferior to lipid-based ready-to-use supplementary foods for the treatment of moderate acute malnutrition in Malawian children. *Am J Clin Nutr.* 2012; 95:212–219. [PubMed: 22170366]
- Medica DL, Sinnis P. Quantitative dynamics of *Plasmodium yoelii* sporozoite transmission by infected anopheline mosquitoes. *Infect Immun.* 2005; 73:4363–4369. [PubMed: 15972531]

- Morris TW, Reed KE, Cronan JE Jr. Identification of the gene encoding lipoate-protein ligase A of *Escherichia coli*. Molecular cloning and characterization of the *lplA* gene and gene product. *J Biol Chem*. 1994; 269:16091–16100. [PubMed: 8206909]
- Mueller AK, Camargo N, Kaiser K, Andorfer C, Frevert U, Matuschewski K, Kappe SH. *Plasmodium* liver stage developmental arrest by depletion of a protein at the parasite-host interface. *Proc Natl Acad Sci U S A*. 2005a; 102:3022–3027. [PubMed: 15699336]
- Mueller AK, Labaied M, Kappe SH, Matuschewski K. Genetically modified *Plasmodium* parasites as a protective experimental malaria vaccine. *Nature*. 2005b; 433:164–167. [PubMed: 15580261]
- Nguyen UT, Goody RS, Alexandrov K. Understanding and exploiting protein prenyltransferases. *Chembiochem*. 2010; 11:1194–1201. [PubMed: 20432425]
- Olszewski KL, Mather MW, Morrissey JM, Garcia BA, Vaidya AB, Rabinowitz JD, Llinas M. Branched tricarboxylic acid metabolism in *Plasmodium falciparum*. *Nature*. 2010; 466:774–778. [PubMed: 20686576]
- Packer L, Cadenas E. Lipoic acid: energy metabolism and redox regulation of transcription and cell signaling. *J Clin Biochem Nutr*. 2011; 48:26–32. [PubMed: 21297908]
- Pei Y, Tarun AS, Vaughan AM, Herman RW, Soliman JM, Erickson-Wayman A, Kappe SH. *Plasmodium* pyruvate dehydrogenase activity is only essential for the parasite's progression from liver infection to blood infection. *Mol Microbiol*. 2010; 75:957–971. [PubMed: 20487290]
- Perham RN. Swinging arms and swinging domains in multifunctional enzymes: catalytic machines for multistep reactions. *Annu Rev Biochem*. 2000; 69:961–1004. [PubMed: 10966480]
- Posluszny JA Jr, Muthumalaiappan K, Kini AR, Szilagyi A, He LK, Li Y, et al. Burn injury dampens erythroid cell production through reprioritizing bone marrow hematopoietic response. *J Trauma*. 2011; 71:1288–1296. [PubMed: 22071930]
- Price RN, Uhlemann AC, Brockman A, McGready R, Ashley E, Phaipun L, et al. Mefloquine resistance in *Plasmodium falciparum* and increased *pfmdr1* gene copy number. *Lancet*. 2004; 364:438–447. [PubMed: 15288742]
- Prudencio M, Rodriguez A, Mota MM. The silent path to thousands of merozoites: the *Plasmodium* liver stage. *Nat Rev Microbiol*. 2006; 4:849–856. [PubMed: 17041632]
- Ralph SA, van Dooren GG, Waller RF, Crawford MJ, Fraunholz MJ, Foth BJ, et al. Tropical infectious diseases: metabolic maps and functions of the *Plasmodium falciparum* apicoplast. *Nat Rev Microbiol*. 2004; 2:203–216. [PubMed: 15083156]
- Rankin KE, Graewe S, Heussler VT, Stanway RR. Imaging liver-stage malaria parasites. *Cell Microbiol*. 2010; 12:569–579. [PubMed: 20180802]
- Saliba KJ, Kirk K. Nutrient acquisition by intracellular apicomplexan parasites: staying in for dinner. *Int J Parasitol*. 2001; 31:1321–1330. [PubMed: 11566300]
- Scheller LF, Wirtz RA, Azad AF. Susceptibility of different strains of mice to hepatic infection with *Plasmodium berghei*. *Infect Immun*. 1994; 62:4844–4847. [PubMed: 7927764]
- Shay KP, Moreau RF, Smith EJ, Smith AR, Hagen TM. Alpha-lipoic acid as a dietary supplement: molecular mechanisms and therapeutic potential. *Biochim Biophys Acta*. 2009; 1790:1149–1160. [PubMed: 19664690]
- Silvie O, Mota MM, Matuschewski K, Prudencio M. Interactions of the malaria parasite and its mammalian host. *Curr Opin Microbiol*. 2008; 11:352–359. [PubMed: 18644249]
- Simmons D, Woollett G, Bergin-Cartwright M, Kay D, Scaife J. A malaria protein exported into a new compartment within the host erythrocyte. *EMBO J*. 1987; 6:485–491. [PubMed: 2438130]
- Spalding MD, Allary M, Gallagher JR, Prigge ST. Validation of a modified method for Bxb1 mycobacteriophage integrase-mediated recombination in *Plasmodium falciparum* by localization of the H-protein of the glycine cleavage complex to the mitochondrion. *Mol Biochem Parasitol*. 2010a; 172:156–160. [PubMed: 20403390]
- Spalding MD, Prigge ST. Lipoic acid metabolism in microbial pathogens. *Microbiol Mol Biol Rev*. 2010b; 74:200–228. [PubMed: 20508247]
- Stanway RR, Witt T, Zobiak B, Aepfelbacher M, Heussler VT. GFP-targeting allows visualization of the apicoplast throughout the life cycle of live malaria parasites. *Biol Cell*. 2009; 101:415–430. 415 p following 430. [PubMed: 19143588]

- Storm J, Muller S. Lipoic acid metabolism of *Plasmodium* - a suitable drug target. *Curr Pharm Des*. 2012; 18:3480–3489. [PubMed: 22607141]
- Sturm A, Graewe S, Franke-Fayard B, Retzlaff S, Bolte S, Roppenser B, et al. Alteration of the parasite plasma membrane and the parasitophorous vacuole membrane during exo-erythrocytic development of malaria parasites. *Protist*. 2009; 160:51–63. [PubMed: 19026596]
- Tarun AS, Peng X, Dumpit RF, Ogata Y, Silva-Rivera H, Camargo N, et al. A combined transcriptome and proteome survey of malaria parasite liver stages. *Proc Natl Acad Sci U S A*. 2008; 105:305–310. [PubMed: 18172196]
- Tonkin CJ, van Dooren GG, Spurck TP, Struck NS, Good RT, Handman E, et al. Localization of organellar proteins in *Plasmodium falciparum* using a novel set of transfection vectors and a new immunofluorescence fixation method. *Mol Biochem Parasitol*. 2004; 137:13–21. [PubMed: 15279947]
- van Dijk MR, Douradinha B, Franke-Fayard B, Heussler V, van Dooren MW, van Schaijk B, et al. Genetically attenuated, P36p-deficient malarial sporozoites induce protective immunity and apoptosis of infected liver cells. *Proc Natl Acad Sci U S A*. 2005; 102:12194–12199. [PubMed: 16103357]
- van Dooren GG, Marti M, Tonkin CJ, Stimmler LM, Cowman AF, McFadden GI. Development of the endoplasmic reticulum, mitochondrion and apicoplast during the asexual life cycle of *Plasmodium falciparum*. *Mol Microbiol*. 2005; 57:405–419. [PubMed: 15978074]
- Vaughan AM, O'Neill MT, Tarun AS, Camargo N, Phuong TM, Aly AS, et al. Type II fatty acid synthesis is essential only for malaria parasite late liver stage development. *Cell Microbiol*. 2009; 11:506–520. [PubMed: 19068099]
- Victoria CG, Adair L, Fall C, Hallal PC, Martorell R, Richter L, Sachdev HS. Maternal and child undernutrition: consequences for adult health and human capital. *Lancet*. 2008; 371:340–357. [PubMed: 18206223]
- Waller RF, Reed MB, Cowman AF, McFadden GI. Protein trafficking to the plastid of *Plasmodium falciparum* is via the secretory pathway. *The EMBO journal*. 2000; 19:1794–1802. [PubMed: 10775264]
- Whelock CE, Goto S, Hammock BD, Newman JW. Clofibrate-induced changes in the liver, heart, brain and white adipose lipid metabolome of Swiss-Webster mice. *Metabolomics*. 2007; 3:137–145. [PubMed: 19079556]
- WHO. World Malaria Report 2012. 2012. http://www.who.int/malaria/publications/world_malaria_report_2012/report/en/index.html
- Wrenger C, Muller S. The human malaria parasite *Plasmodium falciparum* has distinct organelle-specific lipoylation pathways. *Mol Microbiol*. 2004; 53:103–113. [PubMed: 15225307]
- Yamauchi LM, Coppi A, Snounou G, Sinnis P. *Plasmodium* sporozoites trickle out of the injection site. *Cell Microbiol*. 2007; 9:1215–1222. [PubMed: 17223931]
- Yeh E, DeRisi JL. Chemical rescue of malaria parasites lacking an apicoplast defines organelle function in blood-stage *Plasmodium falciparum*. *PLoS Biol*. 2011; 9:e1001138. [PubMed: 21912516]
- Yi X, Maeda N. Endogenous production of lipoic acid is essential for mouse development. *Mol Cell Biol*. 2005; 25:8387–8392. [PubMed: 16135825]
- Yu M, Kumar TR, Nkrumah LJ, Coppi A, Retzlaff S, Li CD, et al. The fatty acid biosynthesis enzyme FabI plays a key role in the development of liver-stage malarial parasites. *Cell Host Microbe*. 2008; 4:567–578. [PubMed: 19064257]

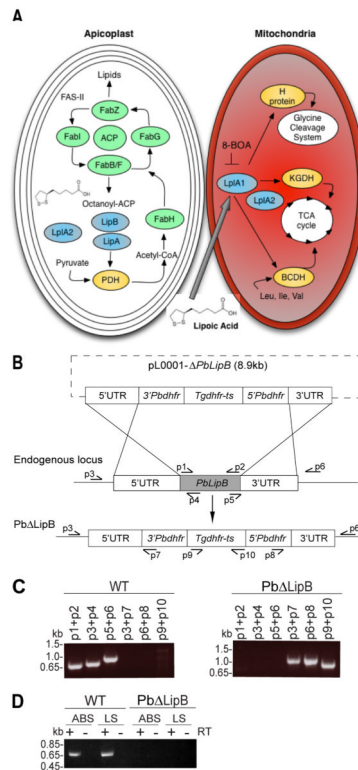


Fig. 1. Generation of *Pb LipB* knockout parasites in *Plasmodium berghei*

A. Schematic representation of lipoids synthesis and scavenging in the *Plasmodium* apicoplast and mitochondrion respectively. Enzymes responsible for the synthesis or attachment of lipoids acid to its target proteins are represented in blue. LipB and LipA synthesize lipoids acid from the octanoyl-acyl carrier protein (ACP) precursor generated by the fatty acid biosynthesis type II (FAS-II) pathway. LipB is responsible for the attachment of octanoyl-ACP to the E-2 subunit of the pyruvate dehydrogenase (PDH) complex within the apicoplast. LipA is responsible for creating the thiosulfur bonds. PDH converts pyruvate into acetyl-CoA, which primes the FAS-II pathway. In the mitochondria, LplA1 attaches scavenged lipoids acid to α -ketoglutarate dehydrogenase (KGDH) and branched-chain α -ketoacid dehydrogenase-E2 subunit (BCDH), which both feed into the tricarboxylic acid (TCA) cycle, as well as the H-protein of the glycine cleavage system. Attachment of scavenged lipoids acid can be inhibited by the analog 8-BOA that targets the ligase LplA1. A second lipoids ligase, LplA2, has been localized to both the apicoplast and the mitochondria.

B. Schematic representation of the replacement strategy used to delete the *PbLipB* gene, based on homologous recombination and double crossover events between the pL0001-*PbLipB* donor plasmid and the *PbLipB* genomic locus.

C. PCR confirmation of the *PbLipB* gene deletion and its replacement with *Tgdhfr-ts*. The left panel shows PCR products specific to the *PbLipB* coding sequence and its 5' and 3' UTRs in the parental *P. berghei* ANKA strain. This showed the expected band sizes of 0.70, 0.76 and 0.98 kb for p1+p2, p3+p4 and p5+p6 respectively. The right panel shows the replacement of *PbLipB* sequence with the *Tgdhfr-ts* marker in a *Pb LipB* knockout clone. This shows the expected band sizes of 1.0, 0.98 and 0.93 kb for p3+p7, p6+p8 and p9+p10 respectively.

D. Reverse transcriptase (RT)-PCR studies showing the loss of *PbLipB* transcription in *Pb LipB* parasites and the expression of this gene in asexual blood stages (ABS) and liver stages (LS) in wild-type (WT) *P. berghei* ANKA parasites. + and - denote with and without RT. Reactions with the LipB-specific primers p1 + p2 showed the expected 0.7 kb

transcription product in WT but not in KO parasites. Control reactions with *P. berghei* actin I-specific primers yielded the expected products with both KO and WT cDNA preparations (data not shown).

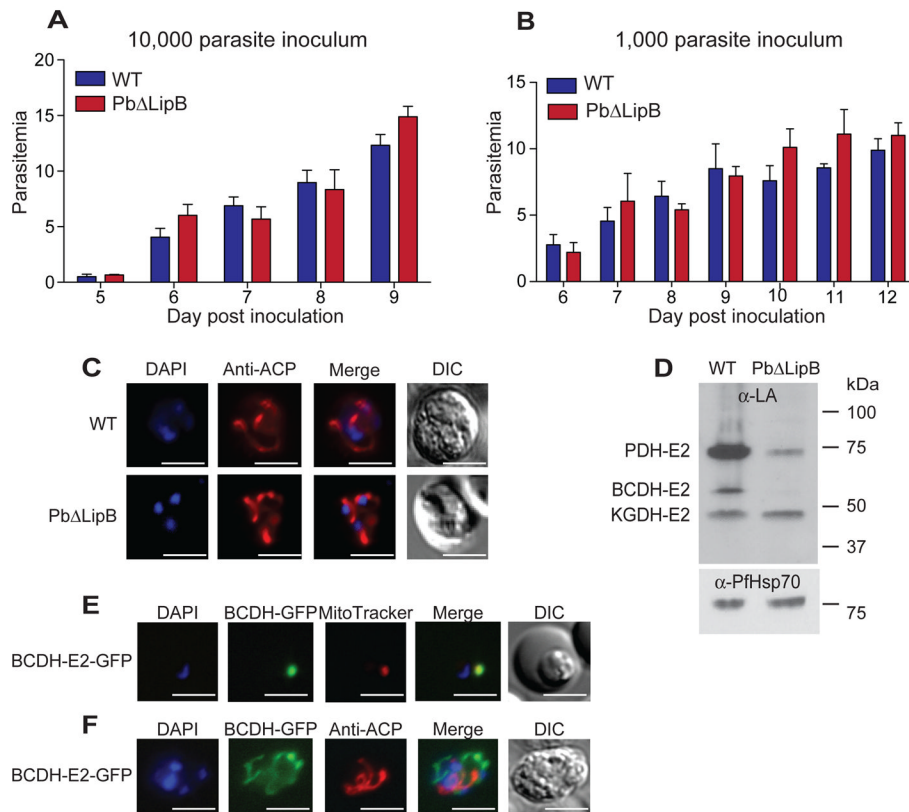


Fig. 2. Pb LipB parasites show normal kinetics of blood stage replication but show reduced lipoylation of parasite dehydrogenases

A, B. Blood stage growth kinetics of Pb LipB and parental wild-type (WT) strains, in mice inoculated with 10,000 or 1,000 asexual blood stage parasites. Five mice were infected with each strain and the experiment performed on three occasions. Mean parasitemias were calculated from each experiment and used to determine the average \pm SEM shown here for each day post-inoculation. Mann-Whitney U tests showed no significant differences in growth kinetics between the two strains.

C. Apicoplast morphology in WT and Pb LipB asexual blood parasites. These parasites were collected from infected mice, allowed to mature overnight *in vitro*, fixed, and stained with ACP-specific antibodies that label the apicoplast as well as DAPI that stains the nucleus. Microscopic examination revealed no significant difference in apicoplast morphology between these strains.

D. Western blot analysis of WT and Pb LipB parasite protein extracts (16 μ g per lane) labeled with antibodies specific to lipoic acid. PDH-E2, pyruvate dehydrogenase E2 subunit; BCDH-E2, branched-chain α -ketoacid dehydrogenase E2 subunit; KGDH-E2, α -ketoglutarate dehydrogenase E2 subunit. The membrane was stripped and re-probed with antibodies specific to *P. falciparum* Hsp70 as a loading control. Data are presented as one representative image from three independent experiments. BCDH-E2 was detected in the Pb LipB parasites at longer exposures (data not shown). Based on band intensity quantification (using ImageJ; NIH), we estimated that lipoylated PDH-E2, BCDH-E2 and KGDH-E2 were present in the LipB-deficient parasite at 16%, 2% and 98% of WT, normalized for loading based on the intensity of Hsp70 labeling.

E. The BCDH-E2 protein localizes to the mitochondria in blood stages. Parasites expressing BCDH-E2-GFP fusion proteins were stained with MitoTracker Red, revealing co-localization with the mitochondrial dye.

F. The BCDH-E2 protein is not localized to the apicoplast. BCDH-E2-GFP parasites were fixed and stained with anti-ACP antibodies to identify the location of the apicoplast, which did not localize with BCDH-E2. White bar, 10 μm (for all panels in this Figure).

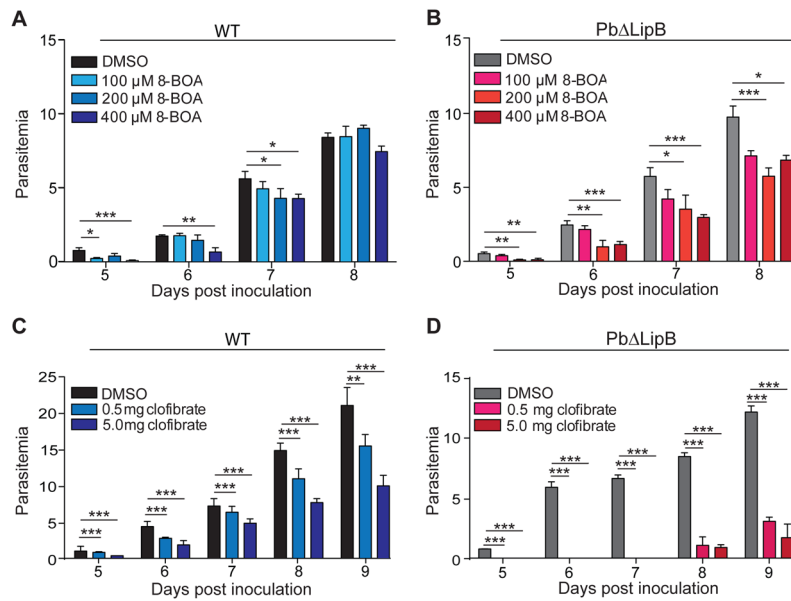


Fig. 3. Blood stage Pb LipB parasites display reduced growth rates following inhibition of lipoid acid scavenging from the host or reduction of host lipid levels with clofibrate

A, B. Effect of 8-BOA on growth rates of LipB KO and WT asexual blood stage parasites. (A) *P. berghei* WT or (B) Pb LipB parasites were treated with concentrations of 100, 200 or 400 μM 8-BOA or DMSO control during overnight *in vitro* incubations, followed by injections of 10,000 parasites into each mouse. Parasitemias were monitored daily, and are presented as means ± SEM of three independent experiments each with 5 mice per group. The 8-BOA treatments showed a dose-dependent effect and a stronger impact on the Pb LipB parasites than on the WT control. Tests for significance employed the Mann-Whitney *U* test that compared parasitemias between the groups of 15 mice injected with parasites that were untreated, versus those injected with parasites treated at a given 8-BOA concentration. * $P < 0.05$; ** $P < 0.01$; *** $P < 0.001$.

C, D. Mice were treated with either 0.5 mg/kg, 5.0 mg/kg of clofibrate or DMSO as vehicle control prior to inoculation with either *P. berghei* ANKA or Pb LipB parasites. Untreated controls showed TG and NEFA mean ± SD concentrations of 0.17 ± 0.03 and 0.16 ± 0.06 mM respectively ($n = 30$). Parasitemias were monitored daily for 9 days and are represented as the averages ± SD of three independent experiments each with 5 mice per group. Statistical tests employed the Mann-Whitney *U* test that compared DMSO-treated controls with each clofibrate concentration. ** $P < 0.01$; *** $P < 0.001$.

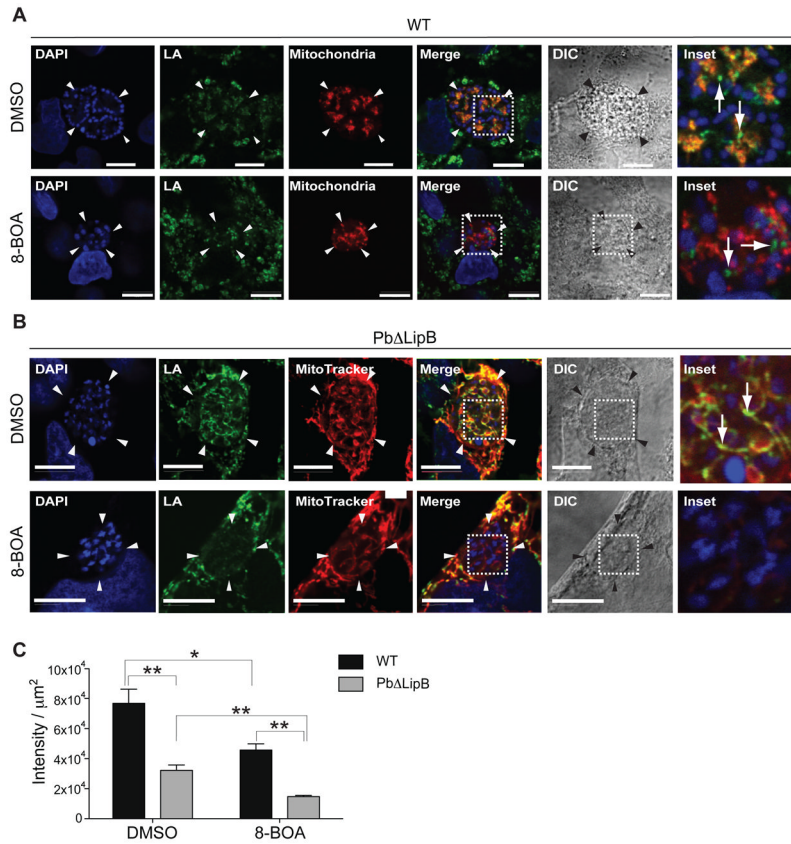


Fig. 4. *Pb LipB* parasites show no residual lipoylated proteins after 8-BOA treatment

A. HepG2 cells were infected with *P. berghei* ANKA mCherry-mito sporozoites and treated with either 200 μM 8-BOA or DMSO as vehicle control. At 54 hpi, infected cells were fixed and stained with anti-lipoic acid (shown in green) to identify lipoylated proteins within the parasite and the HepG2 cell host. The mitochondria is shown in red, while the nucleus (stained with DAPI) is in blue. DIC, differential interference contrast. The dashed white line outlines the portion of the parasite magnified as the Inset in the last column (also for panel B). White bar, 10 μm. White arrows in the inset of WT parasites treated with DMSO control illustrate lipoic acid signal in the mitochondrion (evident as an orange signal).

B. HepG2 cells infected with *Pb LipB* sporozoites were treated with either 200 μM 8-BOA or DMSO as a vehicle control. At 48 hpi, infected cells were stained with MitoTracker Red to label the mitochondria (red). Cells were fixed and stained with anti-lipoic acid to identify lipoylated proteins (shown in green). DAPI dye identified nuclear structures (blue). White bar, 10 μm. The white arrow in the KO parasite treated with DMSO illustrates some lipoic acid signal in the mitochondrion. This signal is largely absent in 8-BOA treated KO parasites.

C. The amount of lipoylated protein within the parasite was quantified using Python and the MATLAB Image Analysis Toolbox and the signal intensity determined from the anti-lipoic acid images, after cropping for parasite-specific areas, for WT and *Pb LipB* parasites treated with 8-BOA or DMSO vehicle control. Data are presented as the mean ± SEM intensity per μm² of parasite. This analysis revealed significant differences between WT and KO parasites, including reduced lipoylation in *Pb LipB* compared to WT parasites following 8-BOA treatment (* $p < 0.05$; ** $p < 0.01$; Mann-Whitney U test; n = 4 to 8 parasites per condition and per strain).

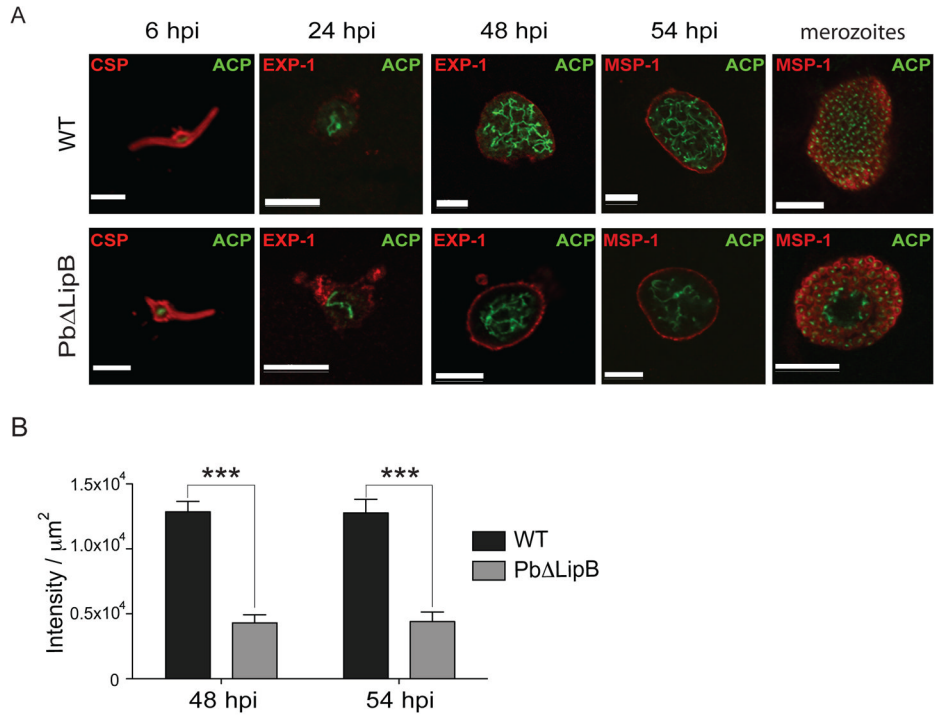


Fig. 5. Pb LipB parasites have a less branched apicoplast in comparison to wild-type cells

A. HepG2 cells were infected with WT or Pb LipB sporozoites and the apicoplast was labeled using ACP-specific antibodies (labeling shown in green) at several time points throughout liver stage development. To visualize the developing parasite, primary antibodies (labeling shown in red) were used as follows: anti-CSP at 6 hpi; anti-Exp-1 at 30 & 48 hpi; anti-MSP-1 at 54 hpi and with mature merozoites (imaged at 62 hpi for WT parasites and 72 hpi for Pb LipB parasites). White bar, 10 μm . B. Plot of intensity of apicoplast staining for WT vs. KO parasites sampled at 48 and 54 hi. Intensity was measured from the anti-ACP image and determined per μm^2 of parasite after cropping the images for the parasite-specific areas (bounded by the parasitophorous vacuole). Results showed a statistically significant two-thirds reduction in apicoplast signal in KO compared to WT parasites (***) ($p < 0.001$; Mann-Whitney U test, $n = 12-18$ per group). Additional images of parasites sampled at 48 and 54 hpi are provided in Figs. S4 and S5 respectively.

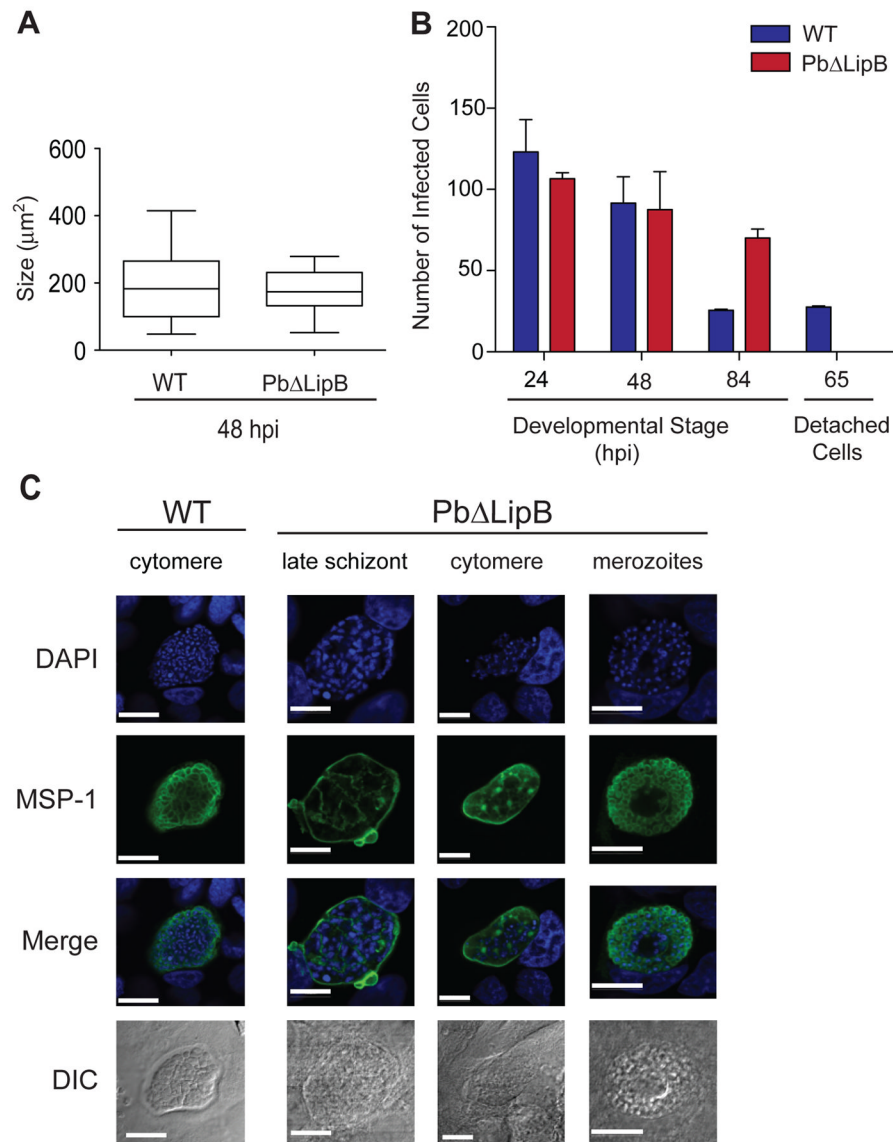


Fig. 6. *Pb LipB* parasites are defective in late liver stage development

A. HepG2 cells were inoculated with either *P. berghei* WT or *Pb LipB* sporozoites, both constitutively expressing GFP. Sizes of developing parasite forms were measured at 48 hpi from 150 to 200 parasites per well (obtained from two independent experiments performed in duplicate) and were quantified using ImageJ. Data are presented as a box and whiskers plot that illustrates the mean, interquartile range (25–75%) and 95% confidence interval.

B. HepG2 cells were infected with equal numbers of WT and KO sporozoites. Parasite numbers were determined by counting fixed and stained developing liver stage parasites, shown for time points 24, 48 and 84 hpi, and counting of live Hoechst-stained detached cells at 65 hpi. Data are shown as the mean \pm SEM generated from two independent experiments performed in duplicate.

C. Liver stage parasites were imaged for DAPI (blue) and MSP-1 (green) expression at different stages of development. The left column shows WT control parasites imaged at the cytomere stage (sampled at 54 hpi). The three right panels show *Pb LipB* liver parasites

developing within HepG2 cells at late schizogony, cytomere and merozoite stages (sampled at 54, 62 and 70 hpi). White bar, 10 μm .

Table 1Pb LipB sporozoites display reduced *in vivo* infectivity.

Experiment	Parasite line	# of Sporozoites Injected	# of Infected Mice	Average Prepatent Period
I	WT	1,000	5 of 5	5.0 days
	Pb LipB	1,000	1 of 5	9.0 days
II	WT	1,000	4 of 4	5.0 days
	Pb LipB	1,000	1 of 4	9.0 days
III	WT	10,000	5 of 5	3.0 days
	Pb LipB	10,000	5 of 5	7.6 days